Hydrodynamic study of fine metallic powders in an original spouted bed contactor in view of chemical vapor deposition treatments

Brigitte Caussat Fernando L. Juarez and Constantin Vahlas

Laboratoire de Génie Chimique (LGC CNRS), ENSIACET/INPT, 5 rue Paulin Talabot, BP1301, 31106 Toulouse Cedex 1, France
Centre Interuniversitaire de Recherche et d'Ingénierie des Matériaux (CIRIMAT CNRS) ENSIACET, 118 Route de Narbonne, 31077 Toulouse cedex 4, France

Abstract

An original gas–solid contactor was developed so as to treat by chemical vapor deposition, fine (mean diameter 23 μm) and dense (bulk density 7700 kg/m^3) NiCoCrAlYTa powders with large size distribution. In order to avoid the presence of a distributor in the reactive zone, a spouted bed configuration was selected, consisting in a glass cylindrical column associated through a 60° cone to an inlet tube, connected at its bottom to a grid so as to support the powders at rest. A hydrodynamic study was conducted at ambient temperature and pressure, combining pressure drop measurements and visual observations as a function of gas velocity and of the ratio H/D of the height of the bed at rest over the bed diameter. Using conventional alumina particles belonging to Geldart's group B, it was shown that this equipment is able to ensure conventional spouted bed behavior, especially for *H*/*D* ratio equal to 1. From numerous experiments conducted with the fine metallic powders of interest, it was shown that (i) conventional pressure drop curves for spouted beds are obtained for *H*/*D* ratios between 1 and 1.8, (ii) due to the large grain size distribution of particles, minimum spouted bed velocities occur in a range rather than at precise values. Visual observations reveal the presence of the spout and fountain at the minimum spouted bed velocity and for H/D equal to 1.

Keywords: Spouted bed; Fluidization; Hydrodynamics; Fine powders; NiCoCrAlYTa powders; MCrAlY powders; Chemical vapor deposition

1. Introduction

In many industrial applications, raw or process materials are fed as powders. Due to their high specific surface area, properties of these powders such as wettability, catalytic activity or behavior in corrosive or oxidative environments mainly depend on the chemical and morphological characteristics of their outer surface layer. Different surface treatment techniques have been developed in order to drive these properties to respond to various engineering requirements and to obtain a final material with required performance. Chemical vapor deposition (CVD) is considered nowadays highly efficient among such techniques, although not yet extensively implemented in industrial environment. CVD is based on relatively simple basic principles: appropriate gaseous species are put in contact with powders in convenient temperature and pressure conditions, so as homogeneous and heterogeneous chemical reactions occur, leading to solid deposition.

To ensure efficient contact between the gaseous CVD precursors and the powders to be treated, CVD operation is classically organized in fluidized bed (FB) reactors or associate technologies (turbulent, circulating or counter current fluidization …). The required activation energy for the chemical reactions to be shifted towards deposition is most often provided by resistively heating the outer walls of the fluidization reactor. In such FBCVD processes, the

design and the positioning of the gas distributor is a hard point, because of the possibility of its plugging up by undesirable precursor decomposition. This question is schematically illustrated by the flow chart of Fig. 1.

Fig. 1. Flow chart illustrating the factors leading to the plugging of the distributor in FBCVD reactors and the possible solutions to this problem. Tdep and Tcond: deposition and precursor condensation temperature, respectively.

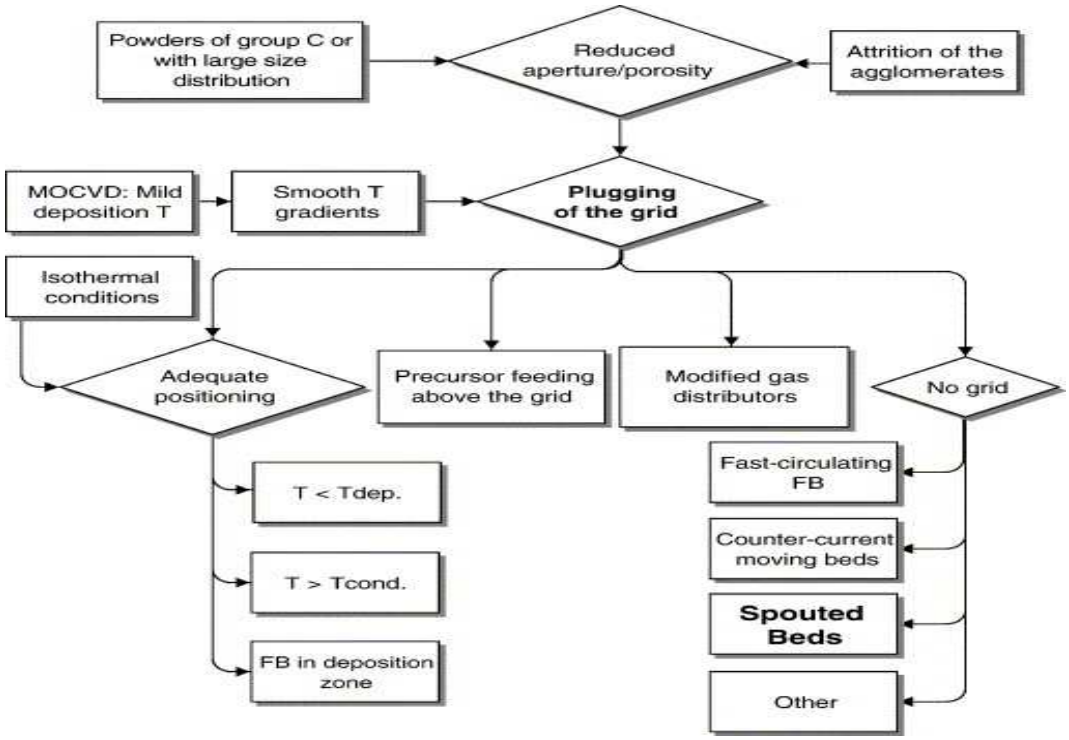

In this figure it is shown that plugging of the grid is subjected to constraints which are more severe when either one or both of the following situations occur: (i) use of powders with low fluidizability; i.e. either belonging to group C of the Geldart classification [1] or presenting a large size distribution with considerable amounts of fines, or being fluidized in the form of agglomerates, (ii) use of molecular or metal organic (MO) precursors in the CVD process. The first point involves the use of distributors or frits with reduced aperture (holes or porosity, respectively). The second one usually concerns solid or liquid compounds at ambient conditions and involves moderate or low operating temperature and, consequently

smooth temperature gradients. Considering the isothermal conditions which prevail in fluidized beds, the distributor in such a case must be placed at a position where (i) the fluidized bed is in the deposition zone and (ii) temperature is both lower than that of deposition or decomposition of the precursor and higher than that of condensation of the precursor.

Due to the difficulty to simultaneously satisfy these constraints for some cases, it has been proposed to directly inject the vaporized precursor in the bed just above the distributor [2], or to appropriately design the reactor not containing any grid or other support to maintain the particles in the deposition zone. An example of such particular CVD reactor designs is the fast circulating fluidized bed. It is characterized by a dilute upward solid flow in the tube center and a fluctuating downward flow of strands of particles at the tube walls. A fast circulating fluidized bed reactor provides low temperature gradients and is suitable for the processing of fine powders at low pressure. Such a setup has been used by Karches et al. to coat in model applications NaCl [3] and soda lime [4] crystals with thin silicon oxide films. In these applications, energy was provided to the system by low temperature plasma, generated in a riser tube by coupling microwaves. Morstein et al. used this technology to deposit ultrathin TiO_2 films on different ceramic powders [5]. Another example of distributor-free CVD process is the counter current moving bed reactor, used by Shinohara and Goldman to coat Si_3N_4 sub-micronic particles with AlN [6]. The authors used $AlCl_3$ and NH_3 gases fed separately at the bottom of the bed, while the powders were introduced through a feeding tank at the top. Rotating drum reactors have also been used for CVD treatments on Geldart's classification group C powders [7]. For more specific applications such as the preparation of a small number of targets for inertial confinement fusion experiments, a piezoelectric system has been used to agitate, in a tapping mode, millimeter-size capsules for their coating with amorphous hydrogenated carbon, by using glow discharge polymerization of CH_4 [8]. Finally, the most simple distributor-free fluidization reactor is the spouted bed (SB) contactor [9] and [10]. In addition to the construction simplicity due to the absence of distributor, SBs are characterized by lower pressure drops and shorter residence time of the gaseous by-products than in classical fluidized beds. On the other hand, they also present disadvantages such as bypassing of gas or possible non-isothermal zones.

SB reactors were originally developed as a method for achieving contact between gas and coarse solid particles belonging to Geldart's group D. They have been associated with

CVD processes since the sixties to coat radioactive particles by pyrolytic carbon and silicon carbide. Considerable progress was achieved in the eighties in this field based on the need to obtain spherical fuel elements with high qualification yield [11]. The accumulated know-how is actually under consideration for the investigation of high temperature gas fuel nuclear reactors [12]. In 1980, in a review on the formation of inorganic coatings from the decomposition of metal organic compounds, Domrachev and Suvorova mentioned the possibility of performing MOCVD in fluidized beds; they provided a scheme combining a precursor evaporator and a spouted bed [13]. No other information was available in the literature until the mid nineties, when Hanabusa et al. [14] and more recently Sanchez et al. [15], reported on the plasma enhanced spouted bed CVD for the deposition of SiC on activated carbon particles and of TiN, Si_3N_4 and SiO_x on silica and corundum particles. Finally, in a patent for the preparation of silicon beads by CVD, the vertical reactor contained multiple zones including an inlet where beads are maintained in a submerged SB [16].

We recently used a spouted bed reactor in a research program aiming the superficial doping with ruthenium and rhenium of as received commercial powders of NiCoCrAlYTa alloys by MOCVD [17], [18], [19] and [20]. Such powders are conventionally air or vacuum plasma sprayed on the surface of gas turbine engine blades and vanes. The coating produced in this way protects the substrate from high temperature oxidation by forming a continuous α-alumina scale. Also, by providing a rough surface, it allows application with improved adhesion of a thermally insulating ceramic top coat composed of yttria stabilized zirconia. Our results revealed that (i) convenient Ru doping of NiCoCrAlYTa coatings by SBCVD increases adhesion of the alumina scale with potential improvement of oxidation resistance, and (ii) since the uniform modification of the composition of commercial raw material is possible by SBCVD, the end user could dispose of a valuable tool to adjust the properties of use as a function of the aimed application. However, to end the validation of this process for the wanted application, the hydrodynamic behavior of such peculiar powders in a lab-scale SB contactor remained to be studied.

Within this frame, the present paper reports on the dimensioning of an original SB reactor and on the investigation and the optimization of the spouting conditions of the NiCoCrAlYTa powders prior their subsequent processing by MOCVD. As it will be shown in the next paragraph, these commercial powders are not prepared in view of fluidization operations. Consequently, their particle size distribution, density, and trend to form

agglomerates, are a priori not convenient for use in a SB or FB reactor. Therefore, it was necessary to determine the parametric window for satisfactory spouting operation in an appropriately designed setup. In that which follows, the physical characteristics of the powders will be presented first. Then, the original design of the reactor will be described then validated by fluidizing conventional alumina particles. Finally, results on the spouting of the metallic powders will be presented and discussed.

2. Experimental

2.1. Powders characteristics

Commercial NiCoCrAlYTa powder (NI-482, Praxair) is a pre-alloyed material which is mainly composed of Ni with additions of Co (21 wt.%), Cr (19 wt.%), Al (8 wt.%), Ta (5 wt.%) and Y (1 wt.%). Fig. 2 presents two SEM micrographs of the as received powder illustrating the spherical shape of the particles. Their skeleton density is 7700 kg/m^3, while the apparent untapped density of the powder equals 4300 kg/m^3. Specific surface area was computed from the N_2 adsorption isotherms (recorded at 77 K with a Micrometrics Flowsorb II2300), using the BET method and was found to be 0.83 m^2/g. This low value is characteristic of a non porous material.

Fig. 2. SEM micrographs of NI-482 powders.

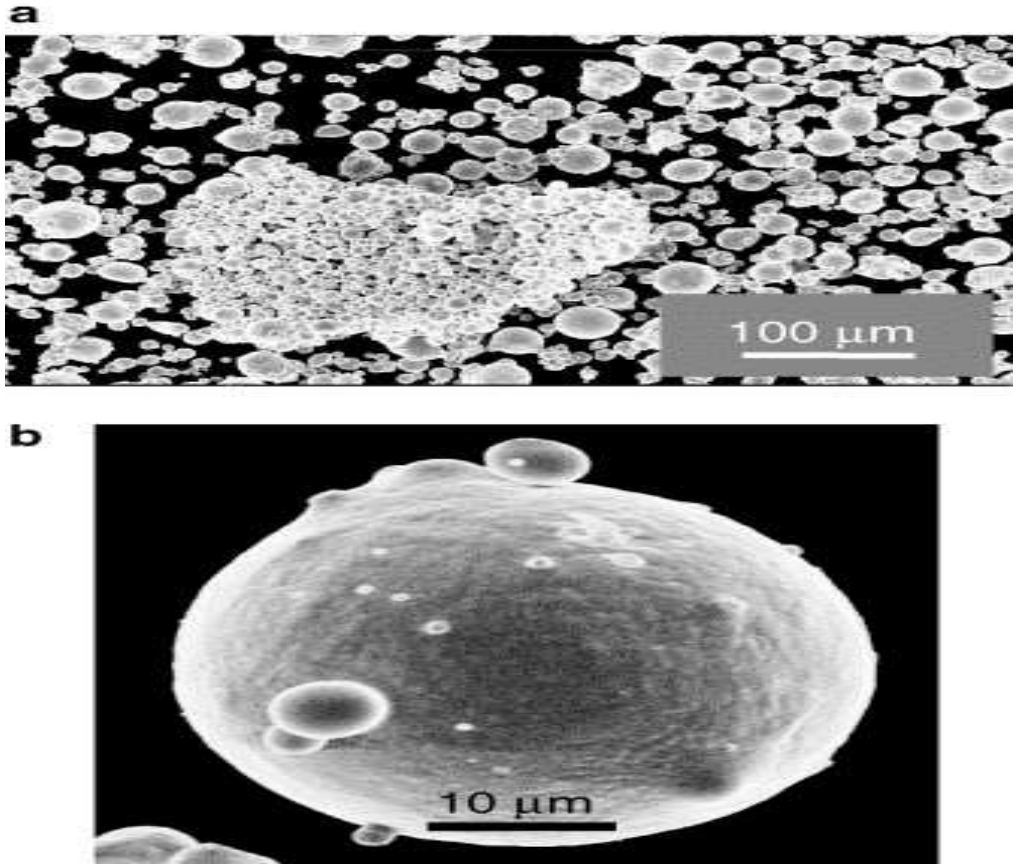

Size distribution was determined with a Malvern Mastersizer laser diffractometer. It was found that mean size distribution of the particles is 23 µm, with minimum 0.05 µm and maximum 556 µm. However, as illustrated in Fig. 2, the largest size corresponds to aggregates rather than to individual particles due to Van der Waals forces. Fig. 3 presents the volume size distribution of the particles, positioned on Geldart's classification diagram [1]. Regarding the Geldart's classification, from the only point of view of the particles size, NI-482 seems to be a mixture of groups C, A and at a lesser extent B powders. Nevertheless, due to its high bulk density, it is placed in extreme position compared to the contours of this chart. NI-482 can thus be qualified as “out” of Geldart's classification. Consequently, homogeneous fluidization of this powder is not a trivial task.

Fig. 3. Volume size distribution of NI-482 powders positioned on Geldart’s diagram [1].

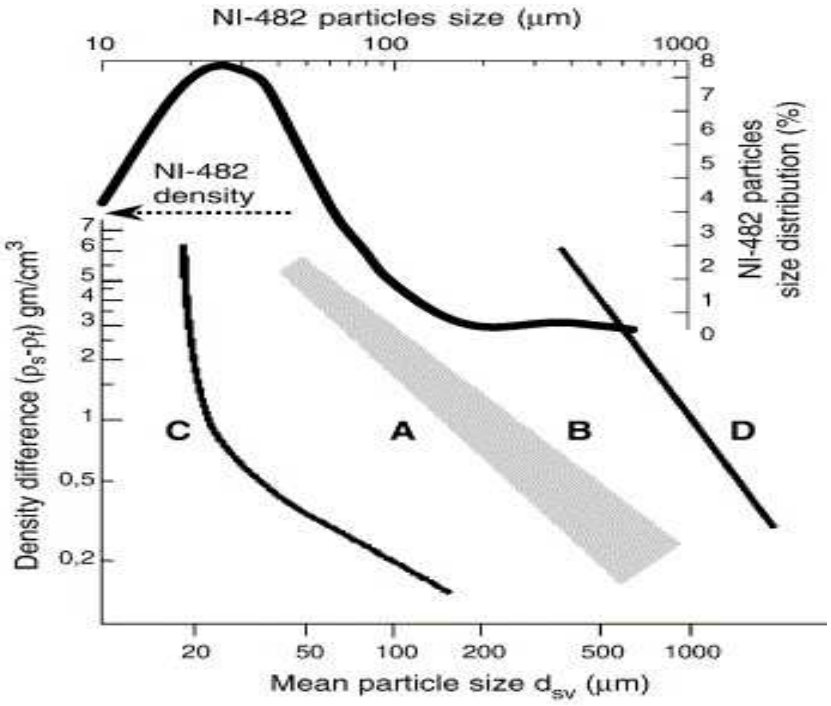

With the hope to facilitate this fluidization, a part of the raw Ni-482 powder has been sieved by sequences of fluidization and elutriation (classical sieving experiments have not been efficient to separate these particles). A batch of sieved powder has thus been prepared, with mean and extreme diameters of 49 μm, and 0.07 and 351 μm, respectively.

2.2. Reactor design

One of the constraints of this study was to treat small quantities of powders, mainly due to the high cost of the involved MO precursors. For this reason, the internal diameter ID of the reactor was limited to 25 mm. The height of the reactor was taken equal to transport disengaging height TDH of the particles. From classical correlations [21], the terminal velocity of powders U_t equals 0.56 and 0.00023 m/s for particles size of 50 and 3 μm, respectively. The design of the reactor was based on the fluidization of 23 μm particles with a U_t = 0.14 m/s. By considering this value and based on the work of Zenz and Weil [22] the ratio TDH/ID equals 25 and TDH equals 630 mm. From these calculations it appears that gas flow values allowing for the fluidization of large or medium size NI-482 lead at the same time to the elutriation of small ones and that, in such a design, elutriation of fines cannot be avoided. To face this problem a 30 cm height and 25 mm ID cylindrical expanded freeboard section was added at the top of the reactor. A bag filter was placed just at the exit of the column so as to collect the elutriated fines.

Different preliminary configurations of the lower part of the reactor, corresponding to the entrance of the gas have been tested in order to define the one schematically illustrated in Fig. 4. The 650 mm height and 25 mm ID glass cylindrical tube is connected at its bottom with a 6 mm ID Pyrex tube, by a 60° conical Pyrex part. This latter diameter was chosen so as all the particles were flowed in the SB column during fluidization. A grid was placed below the cone in order to support the powder at rest. The fluidization gas was dry nitrogen and its flow rate was controlled by two ball rotameters (positioned on feeding lines Q_1 and Q_2 in Fig. 4), operating in the ranges of 200–1000 and 40–290 l/h (Brooks R615A and R215C, respectively). The two rotameters were used simultaneously in parallel operation to investigate more precisely the range of the gas velocity U in the vicinity of the minimum spouted bed velocity U_{ms}. The pressure drop ΔP across the bed, illustrated as the difference (P1–P2) at the corresponding points of Fig. 4, was monitored by a differential pressure transducer (Druck LPX5480) operating in the range 0–2500 Pa with a measurement frequency of 25 Hz. The pressure transducer was connected with a PC computer via a National Instruments NI4350 card. For each flow rate studied, the pressure drop was monitored during 60 s and the arithmetic mean value was calculated to build the classical pressure drop curves; i.e. mean differential pressures versus superficial gas velocity. All measurements were made at decreasing flow rates and at ambient temperature and pressure. Finally, the behavior of the powders in the spouted bed contactor during different steps of their fluidization was visualized and analyzed through digital video camera images.

Fig. 4. Schematic representation of the spouted bed reactor.

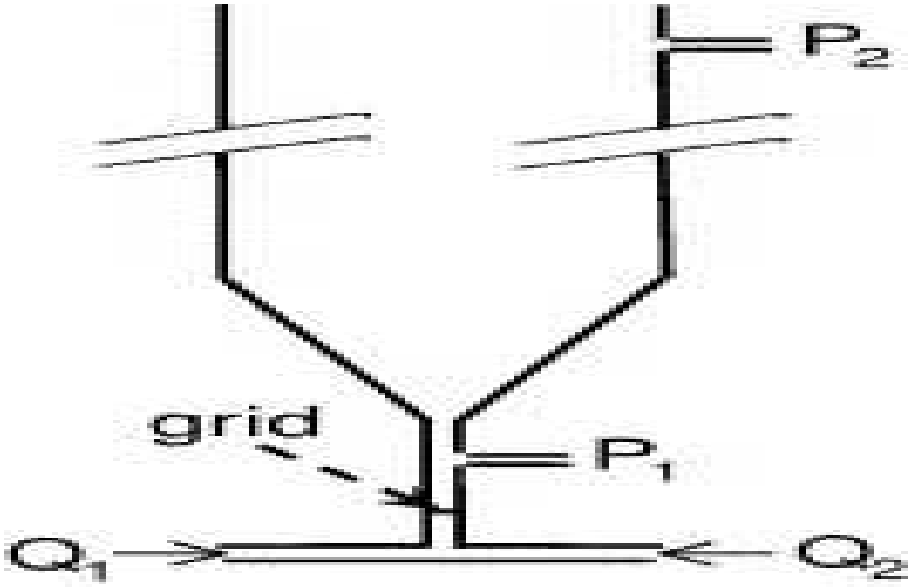

3. Results and discussion

3.1. Validation of the experimental unit

In order to test the SB equipment, in particular regarding the small column diameter, first experiments were conducted with conventional alumina particles (111 μm in mean diameter and 3970 kg/m^3 in bulk density) at different H/D ratios between 1 and 2. Typical two-domain ΔP vs. U curves were obtained, with a steep increase of ΔP at low values of U followed by a plateau above 0.01 m/s. This value was classically taken as the U_{ms} for this system, in good agreement with the literature results for a conventional fluidized bed [21]. The measurements were fully reproducible.

Fig. 5 presents two video images of the alumina SB for H/D = 1 and U/U_{ms} = 1 (5a), and for H/D = 2 and U/U_{ms} = 2 (5b). In the first case the spout is clearly visible, together with the characteristic fountain and annulus regions. For H/D and U/U_{ms} close to 2, a well-defined spout is no more visible, since, on a given section of the cylindrical column, the whole powders are flowed, forming periodic sequences of plugs. The existence of plugging phenomena for U / U_{ms} ratios as low as 2 is due to the very small column diameter,

responsible for high wall effects. These results demonstrate that the parametric range for appropriate operation of this equipment is limited. However, despite its low ID it does ensure a conventional spouted bed behavior, in particular for $H/D = 1$.

Fig. 5. Video snapshots of the alumina spouted beds for $H/D = 1$ and $U/U_{ms} = 1$ (5a), and for $H/D = 2$ and $U/U_{ms} = 2$ (5b).

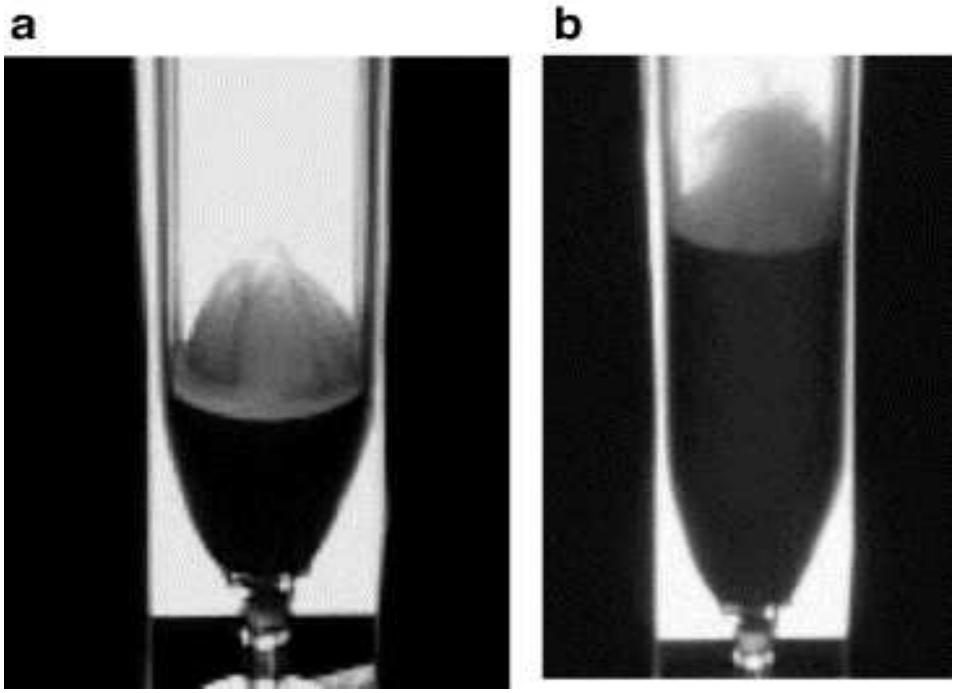

These behaviors have been confirmed by the measurement of temporal evolutions of the differential pressure drop $\Delta P(t)$ for three different gas velocities, lower, equal and higher than U_{ms}. They indicate that the lowest standard deviation occurs for superficial velocities close to U_{ms}. The illustrated behavior corresponds to satisfactory spouting conditions, the powder behaving like a homogeneous medium. For velocities higher than U_{ms}, the fluctuations of pressure drop become more significant, and they seem quite periodic, due to the existence of sequences of plugging. Finally, for gas velocities lower than U_{ms}, the standard deviations are the highest, indicating that the bed is unstable, certainly because of preferential random crossings of gas.

3.2. Investigation of the NiCoCrAlYTa powders

Fig. 6 resumes the obtained results from the spouting of sieved (triangles) and of as received (circles) powders. The results are illustrated in the form of ΔP vs. U curves at decreasing gas velocity, for an initial bed weight of 62 g, corresponding to H/D = 1.5. The general shape of the curve obtained with the sieved powders is characteristic of the powder behavior in a spouted bed. Such a typical curve for spouted beds is presented in the insert of Fig. 6 as proposed in the reference textbook on spouted beds by Mathur and Epstein [9]. Indeed, after a flat zone for the highest gas velocities, a sudden increase of pressure drop appears for a gas velocity corresponding to the minimum spouted bed velocity U_{ms}. Determination of U_{ms} here cannot be very precise since it corresponds to a range of velocities, illustrated by the shaded domain in the diagram, i.e. between 0.02 and 0.029 m/s. This is attributed to the grain size distribution of the powders which, even for the experiment with sieved particles, remains relatively large. Indeed, according to classical correlations of U_{ms} calculation [9], U_{ms} directly depends on the particle diameter. The value of pressure drop corresponding to the spouted bed is located at approximately 1500 Pa. This value is to be compared with the theoretical pressure drop of 1800 Pa corresponding to the apparent bed weight. This difference is attributed to the fact that part of the powders was systematically found either fixed to the walls due to electrostatic forces or elutriated, as it will be discussed thereafter.

Fig. 6. ΔP vs. U at decreasing gas velocity for the as-received (circles) and the sieved (triangles) powders for H/D = 1.5. Temporary fluctuations $\Delta P(t)$, characteristic of three regimes of U: lower, equal and higher than U_{ms}. Insert: typical curve for spouted beds [9].

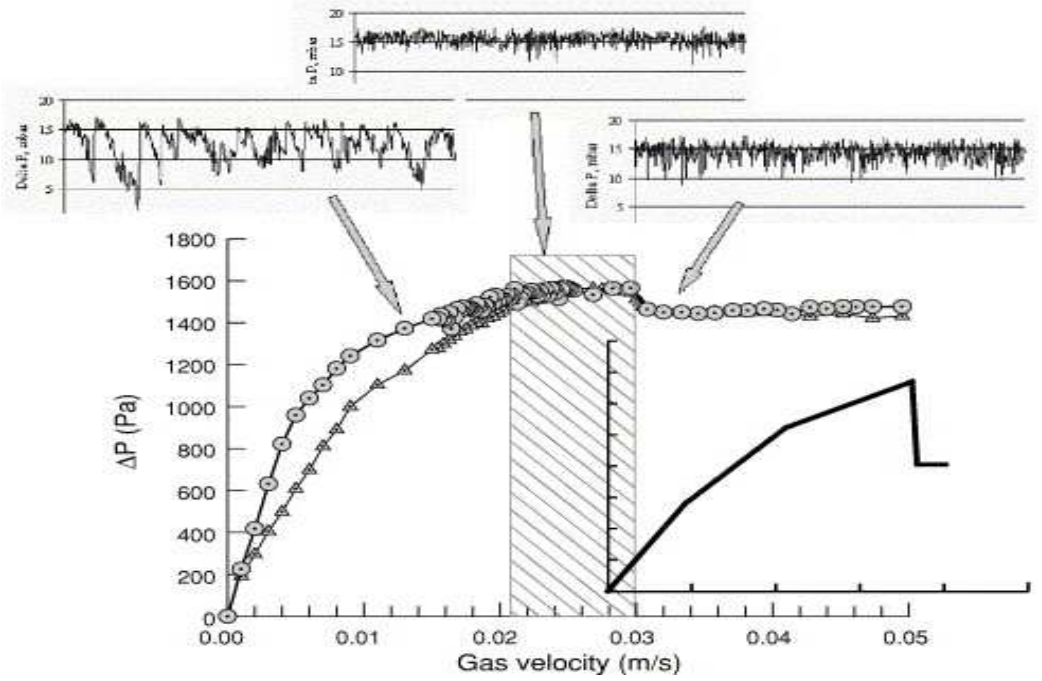

In this figure is also presented the temporal evolution of the differential pressure drop $\Delta P(t)$ of the sieved powders for three different gas velocities, lower, equal and higher than U_{ms}. It is worth noting that the spouting behavior of NiCoCrAlYTa powders is qualitatively similar to that of the previously presented conventional alumina particles, i.e. pressure drops are minimal around U_{ms}, are increased for velocities higher than U_{ms} and are maximum for velocities lower than U_{ms}. A finer analysis through a more frequent sampling of pressure drops would be necessary to investigate the possible periodic character of these fluctuations and thus reveal the exact nature of phenomena occurring in the bed under these conditions.

Finally, Fig. 6 also compares the pressure drop curves between the raw and the sieved powders. As for the sieved ones, U_{ms} of the as received powders corresponds to a range of gas velocities. This range is included between 0.02 and 0.03 m/s; i.e. it is slightly larger than for the sieved powders. However, the main differences between the two ΔP curves occur at gas velocities lower than U_{ms}. In this part of the curves, decrease of ΔP is steeper for the sieved compared with that of raw powders. The observed differences between the two types of powders are attributed to the larger grain size distribution of the raw powders, which enhances their characteristic of mixture of powders with various grain size distributions.

Fig. 7 presents ΔP vs. U curves at decreasing gas velocity for four H/D ratios of the raw powders, namely 1, 1.5, 1.65 and 1.8. All curves have the same general shape except for the

curve at H/D = 1.5 for gas velocities lower than U_{ms}. This behavior is attributed to the intrinsic instability of the bed in this zone as was illustrated by the temporary fluctuation of ΔP reported in Fig. 6. On the other hand, curves present above U_{ms} a stable value of pressure drop which increases with increasing the initial bed weight. This experimental value of ΔP for each H/D ratio is systematically lower than the corresponding theoretical one. The observed difference linearly increases with the value of H/D from 0 to 557 Pa between H/D = 1 and 1.8. As it has already been mentioned, the lower value of the measured ΔP compared with that calculated from the bed weight is mainly attributed to elutriation of the finest particles and to electrostatic pasting of the powders on the column walls. Based on this assumption, the linear increase of the observed difference corresponds to the direct relation of these two phenomena with the initial weight of particles placed into the column.

Fig. 7. ΔP vs. U at decreasing gas velocity for the as-received powders at H/D ratios equal to 1, 1.5, 1.65 and 1.8.

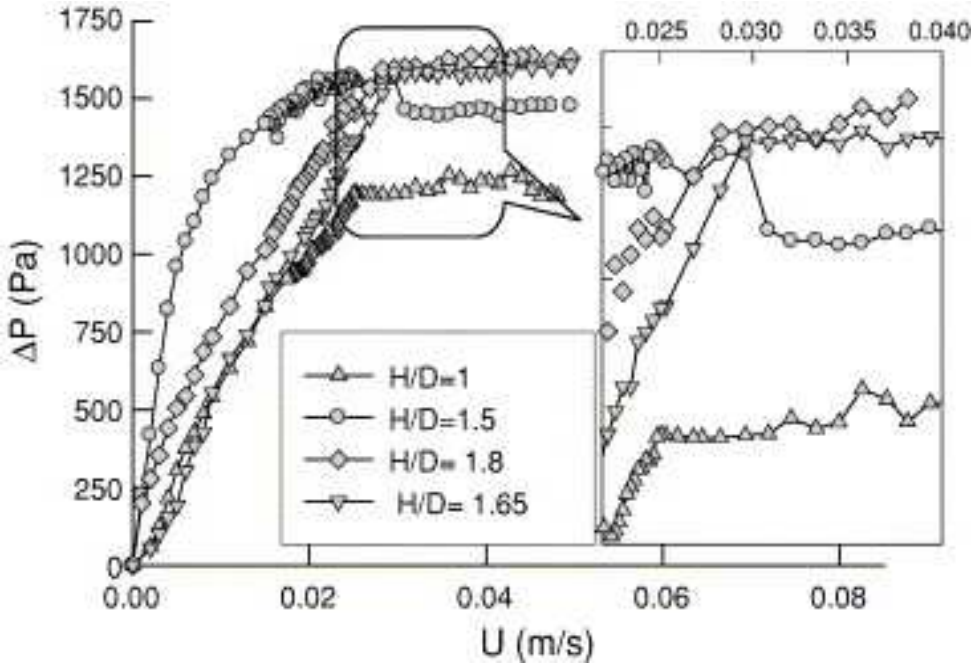

Table 1 resumes the values of U_{ms} for the four H/D ratios as were determined from the curves of Fig. 7. For all but the lowest H/D ratios, U_{ms} corresponds rather to a range of values

than to a precise point. It increases with increasing bed height as is classically observed in spouted beds [9]. The corresponding values of U_{ms} were calculated by the Mathur–Gishler correlation as also reported in Table 1 [23]. This correlation is valid for conventional spouted beds; i.e. millimetric particles of densities lower than 4000 kg/m^3, treated in columns with ID included between 7 mm and 30 cm and for H/D values between 1 and 6. Comparison between experimental and calculated values reveals that the latter overestimate U_{ms} by a factor of 2 to 3. This discrepancy is certainly due to the specific characteristics of the NI-482 powders associated with the low ID of the column; none of the existing correlations of the literature corresponds to the presented parametric range.

Table 1.

Experimental and calculated values of U_{ms} as a function of the H/D ratio

H/D	**1**	**1.5**	**1.65**	**1.8**
Experimental U_{ms} (m/s)	0.025	0.021–0.029	0.03–0.036	0.036–0.041
Calculated U_{ms} (m/s)	0.068	0.083	0.087	0.091

Fig. 8 presents a video image of the spouted bed composed of 53 g of NI-482 raw powders for H/D = 1. This image corresponds to a gas velocity close to U_{ms}, and has been extracted from a decreasing flow rate sequence. The spout and the fountain can be observed, despite the presence of particles pasted on the column walls due to previous intense agitation of the bed at gas velocities considerably higher than U_{ms}.

Fig. 8. Video images of the spouted bed of raw powders at H/D = 1 and U/U_{ms} = 1.

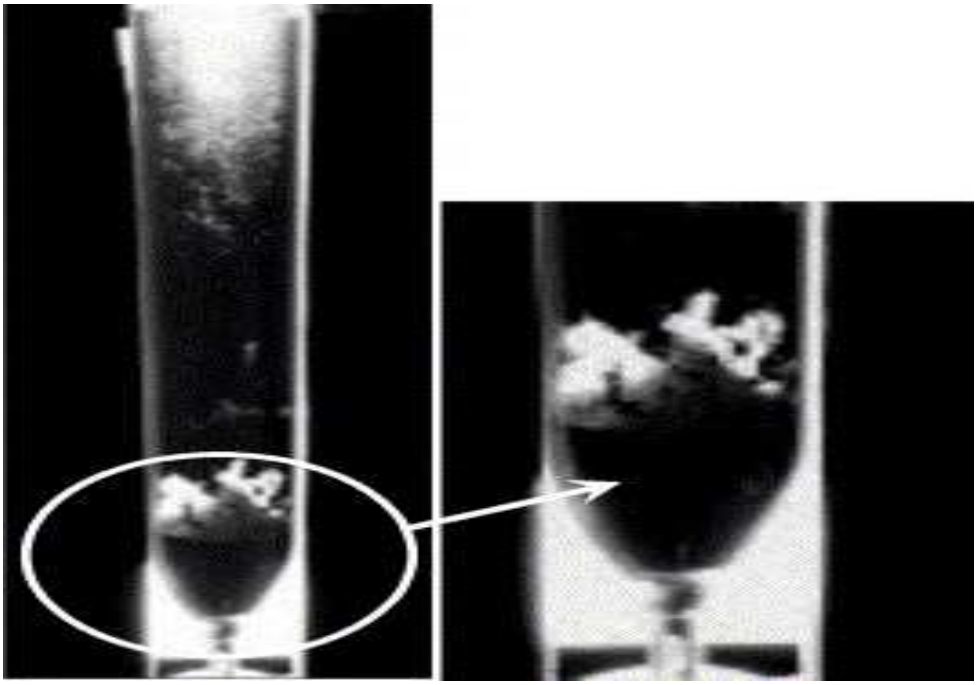

The mechanism of formation of the SB at higher values of H/D is somehow different. For $U < U_{ms}$ the gas crosses the bed through preferential pathways. In some cases, the increase of gas velocity leads to direct formation of the SB through the destruction of such pathways. However, in most cases plugs are formed and this phenomenon is illustrated in the first three video sequences of Fig. 9 illustrating the behavior of the as received powders at $U/U_{ms} = H/D = 2$. In this case, the lower part of the bed is already found in spouting conditions while preferential pathways are formed within the plug. This state is not stable but it is continuously modified; the plug is raised in the reactor (9a), it is reduced (9b) and finally it is destroyed (9c), allowing (i) for the entire quantity of the powder to be fluidized at U near U_{ms} (9d) or (ii) for the formation of chaotic motion at U considerably higher than U_{ms}. These phenomena are characteristic of reactors with reduced diameter. The influence of the walls on the fluidization is too high leading to the formation of plugs and, consequently to incomplete gas–solid contact.

Fig. 9. Video images of the spouted bed of raw powders at $H/D = 2$ and $U/U_{ms} = 2$.

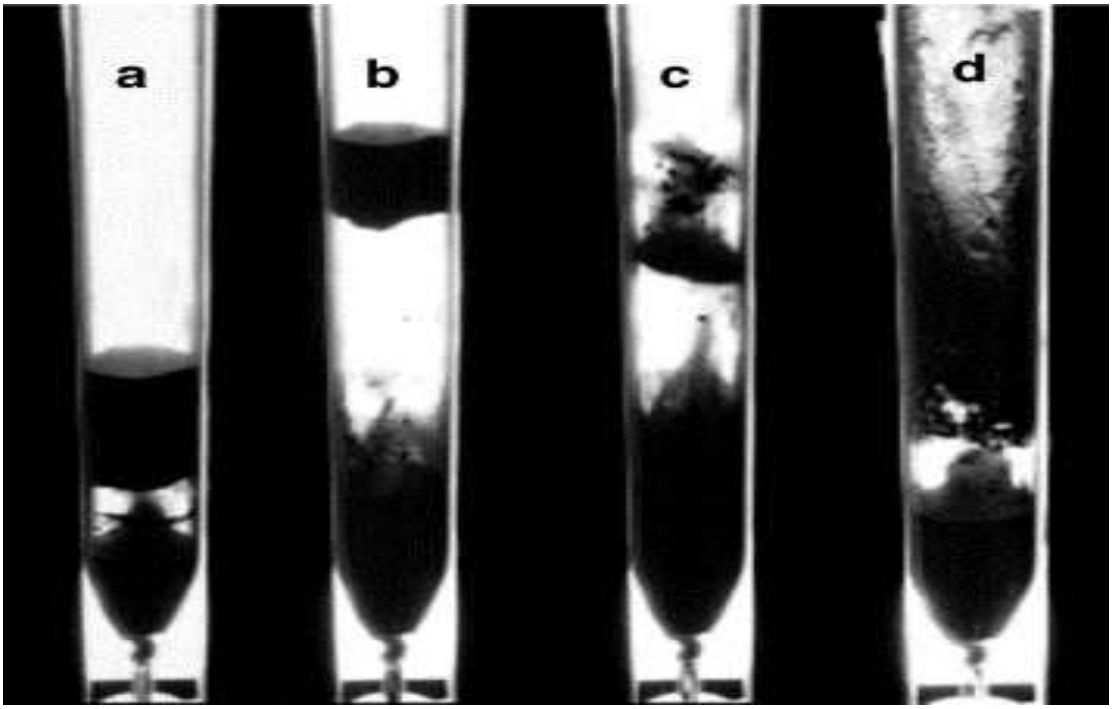

These visual observations indicate that the fluidization of the NI-482 powders in a spouted bed reactor is comparable with, although more difficult than that of alumina ones. The hydrodynamic behavior of NI-482 powders is influenced by their physicochemical nature and their grains size distribution. In any case, these powders can be conveniently fluidized in a spouted bed column of 25 mm ID at least for H/D values near to 1. Of course, the gas–solid contact is certainly not optimal but the possibility of uniformly doping them through a MOCVD treatment is now confirmed. In this latter case, the use of a metallic reactor and the operation at high temperature has attenuated the pasting of the particles to the reactor walls [24] and [25].

In a previous study, by considering appropriate operating conditions, a MOCVD reactor was built in stainless steel to sustain high temperature operation. Only the 2.5 cm ID zone was heated to the metal organic precursor decomposition temperature, and the gaseous precursors were injected from the 6 mm tube [17]. The results obtained for deposition of Ru at 900 K and

Re at 650 K revealed that the deposit was uniform when U/U_{ms} was greater than 1. A priori efficient heat and mass transfers then existed into the bed, probably thanks to convenient spouted bed conditions [17], [19] and [20], as confirmed by the present results. This surface treatment of the NiCoCrAlYTa powders allowed a substantial improvement of the properties of use of the corresponding bond coats [18] and [25].

4. Conclusions

The present study aimed in developing an original gas–solid contactor so as to treat by MOCVD, fine and very dense metallic powders presenting a large grains size distribution. A hydrodynamic study was conducted at ambient temperature and pressure on a 2.5 cm internal diameter spouted bed column. First, using conventional alumina particles belonging to Geldart's group B, it was demonstrated that this equipment is able to ensure conventional spouted bed behavior, especially for an H/D ratio equal to 1. From the numerous experiments conducted with the fine metallic powders of interest the following conclusions were obtained: (i) Conventional pressure drop curves for spouted beds can be obtained for H/D ratios between 1 and 1.8. (ii) Ranges rather than precise values of minimum spouted bed velocities were found, due to the large grains size distribution of particles. (iii) A non negligible part of powders was either pasted on the column walls or elutriated. (iv) Visual observations revealed the presence of the spout and fountain for H/D and U/U_{ms} ratios equal to 1. (v) A comparison with theoretical U_{ms} values calculated from the conventional Mathur–Gishler correlation confirms the peculiarity of the process conditions investigated here. These positive results validate the use of a SB for the superficial doping by Ru and Re of NiCoCrAlYTa powders by MOCVD. It allowed homogenous deposition of the two metals on the surface of the particles. Thermal barrier bond coats obtained from these modified powders showed improved resistance in conditions of cyclic oxidation.

Acknowledgments

We are indebted to M.D. Grenouiller at the Multimedia Service (SCoM) of Paul Sabatier University for video recordings and to M.-C. Duclos and to N. Sussana for their help with the experimental setup. This work was performed through a grant #119553 accorded to FJL by the CONACyT, Mexico with the administrative support of SFERE. The support of the Institut National Polytechnique de Toulouse through a “Bonus Qualité Recherche” action is also acknowledged.

References

D. Geldart, *Powder Technol.* 7 (1973), p. 285.

S. Morooka, A. Kobata and K. Kusakabe, *AIChE Symp. Ser.* 281, 87 (1991), p. 32.

M. Karches, C. Bayer and P.R. v. Rohr, *Surf. Coat. Technol.* 116–119 (1999), p. 879.

M. Karches and P.R. von Rohr, *Surf. Coat. Technol.* 142–144 (2001), p. 28.

M. Morstein, M. Karches, C. Bayer, D. Casanova and P.R. V. Rohr, *Chem. Vap. Depos.* 6 (2000), p. 16.

K. Shinohara, B. Golman, K. Watanabe and S. Chiba, *J. Chem. Eng. Jpn.* 30 (1997), p. 514.

H. Itoh, N. Watanabe and S. Naka, *J. Mater. Sci.* 23 (1988), p. 43.

B. Dumay. PhD Thesis, Université de Bourgogne, Dijon, France (2002).

K.B. Mathur and N. Epstein, Spouted Beds, Academic Press, Inc., London (1974).

M. Olazar, S. Alvarez, R. Aguado and M.J.S. José, *Chem. Eng. Technol.* 26 (2003), p. 845.

W. Heit, H. Huschka, W. Rind and G.G. Kaiser, *Nucl. Technol.* 69 (1985), p. 44.

K. Sawa, S. Suzuki and S. Shiozawa, *Nucl. Eng. Des.* 208 (2001), p. 305.

G.A. Domrachev and O.N. Suvorova, *Rus. Chem. Rev.* 49 (1980), p. 810.

T. Hanabusa, S. Uemiya and T. Kojima, *Surf. Coat. Technol.* 88 (1996), p. 226.

I. Sanchez, G. Flamant, D. Gauthier, R. Flamand, J.M. Badie and G. Mazza, *Powder Technol.* 120 (2001), p. 134.

S.M. Lord, R.J. Milligan. US Patent 5,810,934 (1998).

F. Juarez, A. Castillo, B. Pieraggi and C. Vahlas, *J. Phys., IV* 11 (2001), p. 1117.

F. Juarez, D. Monceau, D. Tetard, B. Pieraggi and C. Vahlas, *Surf. Coat. Technol.* 163–164 (2003), p. 44.

F. Juarez, M.-C. Lafont, F. Senocq and C. Vahlas, *Electrochem. Soc. Proc.* 08 (2003), p. 538.

M.C. Lafont, F.J.L. and C. Vahlas, *Scr. Mater.* 51 (2004), p. 699.

D. Kunii and O. Levenspiel, Fluidization Engineering, Butterworth–Heinemann, Stoneham MA (1991).

F.A. Zenz and N.A. Weil, *AIChE J.* 4 (1958), p. 472.

K.B. Mathur and N. Epstein, *Can. J. Chem. Eng.* 52 (1974), p. 129.

P. Lettieri, J.G. Yates and D. Newton, *Powder Technol.* 110 (2000), p. 117.

F. Juarez. PhD Thesis, Institut National Polytechnique. Toulouse, France (2002).

Corresponding author. Tel.: +33 562 885 670; fax: +33 562 885 600.

Original text : Elsevier.com